



Experimental and Numerical Investigation of the Effect of Vertical Axis Wind Turbine Blade Cascading on the Dynamic Stall Phenomenon

By

Amr Ahmed Ahmed El-Feky

A Thesis Submitted to the

Faculty of Engineering at Cairo University

In Partial Fulfillment of the

Requirements for the Degree of

DOCTOR OF PHILOSOPHY

IN

AEROSPACE ENGINEERING

**FACULTY OF ENGINEERING, CAIRO UNIVERSITY
GIZA, EGYPT
2019**



Experimental and Numerical Investigation of the Effect of Vertical Axis Wind Turbine Blade Cascading on the Dynamic Stall Phenomenon

By

Amr Ahmed Ahmed El-Feky

A Thesis Submitted to the

Faculty of Engineering at Cairo University

In Partial Fulfillment of the

Requirements for the Degree of

DOCTOR OF PHILOSOPHY

IN

AEROSPACE ENGINEERING

Under the Supervision

Of

**Prof. Dr. Ibrahim Mohamed Ali
Shabaka**

Professor, Aerospace Department

Faculty of Engineering-Cairo University

**Prof. Dr. Mahdy Taha El Sayed
Badawy**

Professor, Mechanical Department

National Research Center, Dokki, Giza, Egypt

**FACULTY OF ENGINEERING, CAIRO UNIVERSITY
GIZA, EGYPT
2019**

**Experimental and Numerical Investigation of the Effect
of Vertical Axis Wind Turbine Blade Cascading on the
Dynamic Stall Phenomenon**

By

Amr Ahmed Ahmed El-Feky
A Thesis submitted to the
Faculty of Engineering at Cairo University
In Partial Fulfillment of the
Requirements for the Degree of
DOCTOR OF PHILOSOPHY
In
Aerospace Engineering

Approved by the Examining Committee:

Prof. Dr. Ibrahim Mohamed Ali Shabaka (Thesis Main Advisor)

Professor- Aerospace Department- Faculty of Engineering- Cairo University

Prof. Dr. Mahdy Taha Badawy (Advisor)

Professor- Mechanical Engineering Department- National Research Centre- Egypt

Prof. Dr. Ali Abd El Fattah Hashim (Internal Examiner)

Professor- Aerospace Department- Faculty of Engineering- Cairo University

Prof. Dr. Ossama Ezzat Abd El-Elatif (External Examiner)

Mechanical Engineering Department- Faculty of Engineering- Benha University

FACULTY OF ENGINEERING, CAIRO UNIVERSITY

GIZA, EGYPT

2019

Engineer's Name: Amr Ahmed Ahmed El-Feky

Date of Birth: 25/11/1986

Nationality: Egyptian

E-mail: amr.elfeky@gmail.com

Phone: +2 01066805995

Address: NRC, El-Buhouth St., Dokki, Giza

Registration Date: 1/3/2015

Awarding Date: 2019

Degree: Doctor of Philosophy

Department: Aerospace Engineering

Supervisors:

Prof. Dr. Ibrahim Mohamed Ali shabaka

Prof. Dr. Mahdy Taha El-Sayed Badawy

(Mechanical Engineering Dept., National Research Centre)

Examiners:

Prof. Dr. Ossama Ezzat Abd El-Latif (External Examiner)

(Mechanical Engineering Dept – Faculty of Engineering- Benha University)

Prof. Dr. Ali Abd El-Fattah Hashim (Internal Examiner)

Prof. Dr. Ibrahim Mohamed Ali shabaka (Thesis Main Advisor)

Prof. Dr. Mahdy Taha El-Sayed Badawy (Advisor)

(Mechanical Engineering Dept., National Research Centre)

Title of Thesis: “Experimental and Numerical Investigation of the Effect of Vertical Axis Wind Turbine Blade Cascading on the Dynamic Stall Phenomenon”

Key Words: Lift and Drag Coefficients, Oscillating airfoil, VAWT, Dynamic Stall, NACA Airfoils.

Summary:

The study is began with a wide numerical investigation on the deep dynamic stall phenomenon of unsteady flow around oscillating NACA 0012 airfoil at low Reynolds number. The numerical work uses two experimental cases for validating the predicted hysteresis loops and flow structure. The investigation is performed by solving the Navier-Stokes equations with three turbulence models Spalart-Allmaras, $k\epsilon$ -Realizable and $k\omega$ -SST. The results show that the $k\omega$ -SST is a good model for predicting the dynamic stall stages especially the detecting of leading edge vortex (LEV) and post stall shedding comparing to the experimental data. Comparison between static and dynamic situation is performed. Effects of reduced frequency and oscillation amplitude, effects of airfoil thickness and effects of wing end plates on the dynamic stall phenomenon are studied. Fifteen cascading configuration are studied under the same operating conditions including upper cascading, upper forward cascading, and lower forward cascading during oscillation motion. Comparison between the overall generated torque with azimuthal angle resulting from the CFD and DMST of VAWT models in Darrieus motion is performed including forward and backward auxiliary airfoils with specific offset distances effects. Three cases of vertical axis wind turbine are tested experimentally in static situation. The first configuration is the conventional VAWT with three straight blades. The second configuration is the same turbine in the first configuration but adding auxiliary blade parallel to the main blade at each arm with offset radial distance $0.27c$ with no forward or backward shifting distance. The last configuration is adding auxiliary blade parallel to the main blade at each arm with offset radial distance $0.27c$ and $0.5c$ backward offset distance. The results show that the last configuration enhances the self-starting capability by increasing the static torque four times more than the conventional configuration. In dynamic situation, the tangential force increases by increasing the inlet wind speed. The increasing in applied load cause the decreasing in the tangential forces produced by each blade. In case of the back ward cascading, significant value of the positive pitching moment is produced over the main blade and increases with increases the turbine rotation. It causes a negative load cells reading however the turbine rotate in clockwise.



Disclaimer

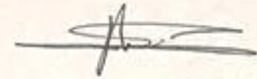
I hereby declare that this thesis is my own original work and that no part of it has been submitted for a degree qualification at any other university or institute.

I further declare that I have appropriately acknowledged all sources used and have cited them in the references section.

Name: Amr Ahmed Ahmed El-Feky

Date: 15/4/2019

Signature:



Dedication

To my Father's soul, **Dr. Ahmed Ahmed El-Feky**, The greatest father and the best friend.

Acknowledgement

I would like to thank all my family, my **Father**, **Mother** and my **Brother** for their encouragement and help during this thesis. I wish for them all the best in their life.

I have greatly appreciated to my supervisor **Prof. Dr. Ibrahim Mohamed Shabaka** for his technical advices, continuous support and redirecting me in the right way during my research.

I would also like to give special thanks to my supervisor **Prof. Dr. Mahdey Taha Badawy** for his help, support and deep revise that added a lot to the value of the work in this thesis.

I would like to express my sincere gratitude to **Dr. Hany El Said Fawaz**, National Research Center; "from whom I learned how to work hard," for his support, and great help in facilitating a lot of difficulties; which faced me throughout this work.

I also would like to express my deepest appreciation to **Prof. Dr. Mohamed Ibrahim El Anwar**, National Research Center; for his valuable guidance, and advices during the course of this work.

I am also owe a heavy debt of gratitude **Prof. Dr. Mohamed Khalil** for his special help and timely support to complete this work.

I cannot express enough thanks to my committee for their continued support and encouragement: **Prof. Dr. Ossama Ezzat Abd Ellatif** and **Prof. Dr. Ali Abd El Fattah Hashim**. I offer my sincere appreciation for the learning opportunities provided by my committee.

The help and encouragement of my friend **Eng. Dyaa El Hak Nabil** is deeply appreciated.

Finally, I wish to acknowledge and express my deep gratitude to all those who helped me in presenting this work.

Table of Contents

Table of Contents	I
List of Tables	V
List of Figures	VI
Abbreviations	XIII
Nomenclature	XV
Abstract	XVI
Chapter 1 Introduction	1
1.1 Motivation	1
1.2 Wind Turbines	1
1.2.1 Types of Vertical Axis Wind Turbine	2
1.2.2 Computational models for Darrieus-type straight-bladed VAWT	3
1.3 The Phenomenon of Dynamic Stall	4
1.3.1 Dynamic stall Stages	5
1.3.2 Parameters affecting Dynamic Stall	7
1.3.2.1 Airfoil Geometry	7
1.3.2.2 Reduced Frequency	8
1.3.2.3 Amplitude and Mean Angle	8
1.3.2.4 Mach Number	9
1.3.2.5 Reynolds Number	9
1.3.2.6 Pitch Axis location	9
1.3.2.7 Three Dimensional Effect	9
1.4 Similarity of Darrieus motion and sinusoidal motion	10
1.5 Thesis outlines	10
Chapter 2 Literature Survey	12
2.1 Overview of Dynamic Stall	12
2.2 Vertical Axis Wind Turbine Dynamic Stall	16
2.3 Dynamic stall Control	17
2.4 Dynamic stall Control using an auxiliary blade	18
2.5 Objectives	19
Chapter 3 Numerical Discretization	20

3.1 Computational Domains and Boundary Conditions	20
3.1.1 2D models	20
3.1.2 3D models	23
3.2 Grid Design	26
3.2.1 2D models	26
3.2.2 3D Models	28
3.3. Numerical Schemes	28
3.3.1 Spalart Allmaras	29
3.3.2 $k\epsilon$ - Realizable	29
3.3.3 $k\omega$ -SST	29
3.4. Case Studies	30
Chapter 4 Numerical Results and Discussion	31
4.1 Model Validation	31
4.1.1 Simulations of case 1	31
4.1.2 Simulations of case 2	32
4.1.3 Mesh and Time Independency Study	34
4.2 Static and Dynamic Situation of Case 2	36
4.3 Effect of Reduced Frequency	39
4.3.1 Sinusoidal motion at $\alpha = 15^\circ + 10^\circ \sin(\omega t)$	39
4.3.2 At Sinusoidal motion: $\alpha = 15^\circ + 15^\circ \sin(\omega t)$	42
4.4 Effect of Airfoil Thickness on the Dynamic Stall	45
4.5 Effect of End Plates on the Dynamic stall Phenomena	47
4.5.1 Dynamic stall over an infinite wing	47
4.5.2 Dynamic stall over a wing with attached tip end plates	47
4.5.3 Dynamic stall over a wing with mounted between two stationary circular plates	50
4.6 Effect of Airfoil cascading on the Dynamic Stall phenomena	53
4.6.1 Upper Cascading	53
4.6.1.1 Upper cascading with 0.25c offset distance	53
4.6.1.2 Upper cascading with 0.5c offset distance	53
4.6.1.3 Upper cascading with 0.75c offset distance	54
4.6.2 Upper Cascading with forward movement 0.25c	58
4.6.2.1 Upper cascading with 0.25c offset distance	58
4.6.2.2 Upper cascading with 0.5c offset distance.	58
4.6.2.3 Upper cascading with 0.75c offset distance	59

4.6.3 Upper Cascading with forward movement 0.5c	63
4.6.3.1 Upper cascading with 0.25c offset distance	63
4.6.3.2 Upper cascading with 0.5c offset distance	63
4.6.3.3 Upper cascading with 0.75c offset distance	64
4.6.4 Lower Cascading with forward movement 0.25c	68
4.6.4.1 Lower cascading with 0.25 offset distance	68
4.6.4.2 Lower cascading with 0.5 offset distance	68
4.6.4.3 Lower cascading with 0.75 offset distance	69
4.6.5 Lower Cascading with forward movement 0.5c	73
4.6.5.1 Lower cascading with 0.25 offset distance	73
4.6.5.2 Lower cascading with 0.5 offset distance	74
4.6.5.3 Lower cascading with 0.75 offset distance	74
4.6.6 Effect of oscillation amplitude on the cascading behavior during the dynamic stall	79
4.6.6.1 Upper cascading with 0.5c offset distance.	79
4.6.6.2 Lower cascading with 0.5c offset distance	79
4.6.6.3 Upper cascading with 0.75c offset distance	80
4.7 2D Airfoils in Darrieus motion	84
4.7.1 Single Row VAWT	84
4.7.2 Forward Cascading VAWT	84
4.7.3 Backward Cascading VAWT	85
Chapter 5 Experimental Setup and Results	99
5.1 Wind Tunnel Facility	99
5.1.1 Data acquisition USB-6218 kit	99
5.1.2 Traverse mechanism	100
5.1.3 Wind tunnel air velocity measurement	100
5.1.4 Flow Temperature measurement	101
5.4.5 Measuring the Turbulence Intensity flow of the wind tunnel	101
5.4.6 Wind Tunnel fan RPM indicator	103
5.2 Vertical Axis Wind Turbine Model	105
5.2.1 Base Flange and Bolt alignment Flange	105
5.2.2 Base holder of pneumatic actuator holder	105
5.2.3 Break Disk	105
5.2.4 Shaft and Bearing Holder	107
5.2.5 Bearing Housing	107

5.2.6 Shaft Encoder Flange	107
5.2.7 Rotor Hub	108
5.2.8 Load Cell Holders	108
5.2.9 Blades Manufacturing	108
5.2.10 Blade cascading rod holders	110
5.2.11 Electronic Circuit	110
5.2.12 Pneumatic Circuit	115
5.3 Static and Dynamic Tests Situations of the VAWT wind tunnel models	117
5.3.1 Single Row Straight blade VAWT	117
5.3.2 Double Rows Straight blade VAWT	118
5.3.2 Double Rows Straight blade VAWT with backward offset distance	119
5.4 Experimental Results of tested wind tunnel models in static situation	121
5.4.1 Single Row Straight blade VAWT	121
5.4.2 Double Rows Straight blade VAWT	122
5.4.3 Double Rows with backward offset distance Straight blade VAWT	122
5.5 Experimental Results of tested wind tunnel models in dynamic situation	128
5.5.1 Dynamic test for Single Row Straight blade VAWT	128
5.5.2 Double Rows with backward offset distance Straight blade VAWT	133
Chapter 6 Conclusions and Future Work	136
6.1 Conclusions	136
6.2 Future Work	137
References	138
Appendices	148
Appendix A: FLUENT User Defined Function Subroutine	148
Appendix B: Traverse Mechanism Parts and Dimensions	149
Appendix C: GUI Program for logging CTA, Pitot tube, LM35 dz, and Infrared proximity readings	150
Appendix D: Base Flange and the Circular Flange Dimensions	152
Appendix E: Base Holder and Break Disk Dimension	153
Appendix F: Bearing Holder and Shaft Encoder Flange Dimensions	154
Appendix G: Rotor Hub and Load Cell Holders Dimensions	155
Appendix H: Blade Cascading Rods Dimensions	156
Appendix I: IDE code and GUI programs for logging load cells reading in static mode	157
Appendix J: IDE code and GUI programs for logging load cells reading in dynamic mode	160

List of Tables

Table 1.1 Merits of vertical axis wind turbines over horizontal axis wind turbines	2
Table 3.1 The turbine geometrical specification	21
Table 3.2 Gird sizes used in the simulations.	27
Table 4.1 Summary of Dynamic stall occasions at different cascading offset distances.	79
Table 5.1 Single Row VAWT Specifications.....	118
Table 5.2 Double Rows VAWT Specifications.....	119
Table 5.3 Double Rows VAWT Specifications.....	120

List of Figures

Fig. 1.1 Savonius-type VAWT.....	2
Fig. 1.2 Darrieus Type.....	3
Fig. 1.3 Scheme of the rotation of a VAWT at different azimuthal angle	4
Fig. 1.4 blade pitching motion.....	5
Fig. 1.5 Schematic showing the essential flow morphology and the unsteady airloads during the dynamic stall process on an oscillating 2-D airfoil	6
Fig. 1.6 Airfoils used in McCroskey’s study.....	7
Fig. 1.7 Similarity with regard to the dynamic stall mechanics for (a) Darrieus motion (b) Sinusoidal motion.....	10
Fig. 2.1 PIV pictures during upstroke at (a) 22° upstroke (b) 24° upstroke	12
Fig. 2.2 Caricatures of LEV development under three-dimensional test conditions (left) and two dimensional test conditions (right)	13
Fig. 2.3 Evolution of the circulation of leading edge separated vortex for $\theta = 72^\circ, 90^\circ, 108^\circ, 133^\circ$ and 158° at $\lambda=2$	16
Fig. 2.4 3D view of the VAWT with flexible auxiliary vane	19
Fig. 2.5 VAWT with an auxiliary blade	19
Fig. 3.1 Boundary conditions for 2D outer domain.....	21
Fig. 3.2 2D model boundary conditions inner domain for (a) oscillating single airfoil (b) oscillating cascading system.	22
Fig. 3.3 Boundary conditions for 2D VAWT outer domain.....	22
Fig. 3.4 2D VAWT inner domain and boundary conditions for (a) conventional VAWT (b) double rows of airfoils with forward movement VAWT (c) double rows with backward movement VAWT.	23
Fig. 3.5 3D Infinite wing with NACA 0012 airfoil section model boundary conditions for (a) outer domain (b) inner domain.	24
Fig. 3.6 3D wing tips attached end plates model boundary conditions for (a) outer domain (b) inner domain.	25
Fig. 3.7 Wing mounted between tow stationary plates boundary conditions for (a) outer domain (b) inner domain.	25
Fig. 3.8 2D oscillating airfoils gird system (a) Outer domain (b) Mesh around the airfoil trailing edge (c) inner and outer 2D domains (d) Hybrid mesh of inner domain in case of cascading airfoils.	26
Fig. 3.9 VAWT gird system (a) inner and outer 2D domains of VAWT (b) Mesh around airfoil (c) Mesh around the airfoil trailing edge.	27
Fig. 3.10 3D Gird system (a) all domains (b) Sectional mesh for 3D model.	28
Fig. 3.11 Wing sinusoidal motion of case 1 [178] and case 2 [179].	30
Fig. 4.1 Lift and Drag coefficients variation with time of case 1 for the three turbulence models, Spalart Allmaras, $k\epsilon$ - Realizable, and $k\omega$ - SST (a) Lift Coefficient (b) Drag Coefficient.....	31
Fig. 4.2 Comparison of three turbulence models Spalart Allmaras, $k\epsilon$ -Realizable, and $k\omega$ -SST prediction for Lift and Drag coefficients with experimental Case 1 (a) Lift coefficient (b) Drag coefficient	32
Fig. 4.3 Stream lines and velocity contours for case 2 for Experimental, Spalart Allmaras, $k\epsilon$ -Realizable and $k\omega$ -SST at angles (a) 22° upstroke (b) 24° upstroke.....	33

Fig. 4.4 Non-dimensional velocity magnitude U/U_∞ at angle 22° upstroke with the nondimensional distance from the blade (a) $x/c=0.25$ (b) $x/c=0.5$ (c) $x/c=0.75$33

Fig. 4.5 Non-dimensional velocity magnitude U/U_∞ at angle 24° upstroke with the nondimensional distance from the blade (a) $x/c =0.25$ (b) $x/c =0.5$ (c) $x/c =0.75$34

Fig. 4.6 Comparison of computed results at various time step sizes $\Delta t = 0.005, 0.003, 0.001, 0.0008$ and 0.0006 for mesh G4 (a) variation of cl with incidence angles (b) Stream lines and velocity contours for case 2 at angle 22° upstroke.35

Fig. 4.7 Comparison of computed results with different grid densities for $\Delta t =0.001$ (a) variation of cl with incidence angles (b) Stream lines and velocity contours for case 2 at angle 22° upstroke.36

Fig. 4.8 Static and dynamic lift and drag coefficients with incidence angle for Case 2 with $K\omega$ -SST scheme (a) lift coefficient (b) drag coefficient.37

Fig. 4.9 Stream lines and velocity magnitude for case 2 in static, upstroke and down stroke situations.39

Fig. 4.10 Stream lines and velocity magnitude for NACA 0012 at reduced frequencies (a) 0.064 (b) 0.085 (c) 0.107 (d) 0.128 (e) 0.15 (f) 0.171 (g) 0.192 (h) 0.214 at incidence angle $\alpha=15^\circ+10^\circ\sin(\omega t)$41

Fig. 4.11 Lift coefficient with incidence angle for NACA 0012 at reduced frequencies 0.064, 0.085, 0.107, 0.128 and 0.15 at incidence angle $\alpha=15^\circ+10^\circ\sin(\omega t)$41

Fig. 4.12 Lift coefficient with incidence angle for NACA 0012 at reduced frequencies 0.15, 0.171, 0.192 and 0.214 at $\alpha=15^\circ+10^\circ\sin(\omega t)$42

Fig. 4.13 Maximum lift coefficient with reduced frequency at $\alpha=15^\circ+10^\circ\sin(\omega t)$42

Fig. 4.14 Stream lines and velocity magnitude for NACA 0012 at reduced frequencies (a) 0.064 (b) 0.085 (c) 0.107 (d) 0.128 (e) 0.15 (f) 0.171 (g) 0.192 (h) 0.214 (i) 0.235 at incidence angle $\alpha=15^\circ+15^\circ\sin(\omega t)$ 44

Fig. 4.15 Lift coefficient with incidence angle for NACA 0012 at reduced frequencies 0.064, 0.085, 0.107, 0.128 and 0.15 at incidence angle $\alpha=15^\circ+15^\circ\sin(\omega t)$44

Fig. 4.16 Lift coefficient with incidence angle for NACA 0012 at reduced frequencies 0.15, 0.171, 0.192, 0.214 and 0.235 at $\alpha=15^\circ+15^\circ\sin(\omega t)$45

Fig. 4.17 Maximum lift coefficient with reduced frequency at $\alpha=15^\circ+15^\circ\sin(\omega t)$45

Fig. 4.18 Stream lines and velocity magnitude for (a) NACA 0010 (b) NACA 0012 (c) NACA 0015 (d) NACA 0018 (e) NACA 0022.46

Fig. 4.19 Lift coefficient with incidence angle for NACA 0010, NACA 0012, NACA 0015, NACA 0018, and NACA 0022.47

Fig. 4.20 Stream lines and pressure contours of oscillating infinite wing of NACA 0012 airfoil section at (a) 22° upstroke (b) 24° upstroke.48

Fig. 4.21 Stream ribbons and pressure contours of oscillating of NACA 0012 airfoil section wing with attached tip end plates at (a) 22° upstroke (b) 24° upstroke.49

Fig. 4.22 Vortex core of oscillating NACA 0012 airfoil section wing with attached tip end plates at (a) 22° upstroke (b) 24° upstroke.49

Fig. 4.23 Velocity magnitude and stream lines of wing lateral sections at angles 22° upstroke and 24° upstroke at (a) $z/c =0.05$ (b) $z/c =0.25$ (c) $z/c =0.5$ (d) $z/c 0.75$ (e) $z/c =0.95$50

Fig. 4.24 Stream ribbons and pressure contours of oscillating of NACA 0012 airfoil section wing with attached tip end plates at (a) 22° upstroke (b) 24° upstroke.51

Fig. 4.25 Velocity magnitude and stream lines of wing mounted between two stationary circular plates lateral sections at angles 22° upstroke and 24° upstroke at (a) $z/c = 0$ (b) $z/c = 0.25$ (c) $z/c = 0.5$ (d) $z/c = 0.75$ (e) $z/c = 1$52

Fig. 4.26 Lift coefficient with incidence angle for Infinite wing, fixed end plates with 1mm wing tip tolerance and attached end plates to wing tip.52

Fig. 4.27 Stream lines and velocity contours of Oscillating two NASA 0012 airfoils with upper cascaded offset distance (a) 0.25c (b) 0.5c (c) 0.75c.....57

Fig. 4.28 Main airfoil lift coefficient in case of upper cascading with offset distance (a) 0.25c (b) 0.5c (c) 0.75c57

Fig. 4.29 Auxiliary airfoil lift coefficient in case of upper cascading with offset distance (a) 0.25c (b) 0.5c (c) 0.75c.....57

Fig. 4.30 Resultant airfoils lift coefficients in case of upper cascading with offset distance (a) 0.25c (b) 0.5c (c) 0.75c.....58

Fig. 4.31 Stream lines and velocity contours of Oscillating two NASA 0012 airfoils with forward movement 0.25c and upper cascaded offset distance (a) 0.25c (b) 0.5c (c) 0.75c.61

Fig. 4.32 Main airfoil lift coefficient in case of upper cascading with forward movement 0.25c and offset distance (a) 0.25c (b) 0.5c (c) 0.75c62

Fig. 4.33 Auxiliary airfoil lift coefficient in case of upper cascading with forward movement 0.25c and offset distance (a) 0.25c (b) 0.5c (c) 0.75c62

Fig. 4.34 Resultant airfoils lift coefficients in case of upper cascading with forward movement 0.25c and offset distance (a) 0.25c (b) 0.5c (c) 0.75c.....63

Fig. 4.35 Stream lines and velocity contours of Oscillating two NASA 0012 airfoils with forward movement 0.5c and upper cascaded offset distance (a) 0.25c (b) 0.5c (c) 0.75c.67

Fig. 4.36 Main airfoil lift coefficient in case of upper cascading with forward movement 0.5c and offset distance (a) 0.25c (b) 0.5c (c) 0.75c67

Fig. 4.37 Auxiliary airfoil lift coefficient in case of upper cascading with forward movement 0.5c and offset distance (a) 0.25c (b) 0.5c (c) 0.75c.67

Fig. 4.38 Resultant airfoils lift coefficients in case of upper cascading with forward movement 0.5c and offset distance (a) 0.25c (b) 0.5c (c) 0.75c.....68

Fig. 4.39 Stream lines and velocity contours of Oscillating two NASA 0012 airfoils with forward movement 0.25c and lower cascaded offset distance (a) 0.25c (b) 0.5c (c) 0.75c.71

Fig. 4.40 Main airfoil lift coefficient in case of upper cascading with forward movement 0.25c and offset distance (a) 0.25c (b) 0.5c (c) 0.75c72

Fig. 4.41 Auxiliary airfoil lift coefficient in case of upper cascading with forward movement 0.25c and offset distance (a) 0.25c (b) 0.5c (c) 0.75c72

Fig. 4.42 Resultant airfoils lift coefficients in case of upper cascading with forward movement 0.25c and offset distance (a) 0.25c (b) 0.5c (c) 0.75c.....73

Fig. 4.43 Stream lines and velocity contours of Oscillating two NASA 0012 airfoils with forward movement 0.25c and lower cascaded offset distance (a) 0.25c (b) 0.5c (c) 0.75c.77

Fig. 4.44 Main airfoil lift coefficient in case of upper cascading with forward movement 0.5c and offset distance (a) 0.25c (b) 0.5c (c) 0.75c77

Fig. 4.45 Auxiliary airfoil lift coefficient in case of upper cascading with forward movement 0.5c and offset distance (a) 0.25c (b) 0.5c (c) 0.75c78

Fig. 4.46 Resultant airfoils lift coefficients in case of upper cascading with forward movement 0.5c and offset distance (a) 0.25c (b) 0.5c (c) 0.75c.....78